Allosteric Linkage between Voltage and Ca^{2+}-Dependent Activation of BK-Type mslo1 K^+ Channels†

Jianmin Cui*,‡ and Richard W. Aldrich§

Department of Biomedical Engineering, Case Western Reserve University, Cleveland, Ohio 44106, and Department of Molecular and Cellular Physiology and Howard Hughes Medical Institute, Stanford University, Stanford, California 94305

Received June 30, 2000; Revised Manuscript Received October 2, 2000

ABSTRACT: The activation of BK type Ca^{2+}-activated K^+ channels depends on both voltage and Ca^{2+}. We studied three point mutations in the putative voltage sensor S4 or S4−S5 linker regions in the mslo1 BK channels to explore the relationship between voltage and Ca^{2+} in activating the channel. These mutations reduced the steepness of the open probability − voltage ($P_o - V$) relation and increased the shift of the $P_o - V$ relations on the voltage axis in response to increases in the calcium concentration. It is striking that these two effects were reciprocally related for all three mutations, despite different effects of the mutations on other aspects of the voltage dependence of channel gating. This reciprocal relationship suggests strongly that the free energy contributions to channel activation provided by voltage and by calcium binding are simply additive. We conclude that the Ca^{2+} binding sites and the voltage sensors do not directly interact. Rather they both affect the mslo1 channel opening through an allosteric mechanism, by influencing the conformational change between the closed and open conformations. The mutations changed the channel's voltage dependence with little effect on its Ca^{2+} affinitiy.

Large conductance Ca^{2+}-activated K^+ channels (BK channels)[1] are activated by membrane depolarization and by the binding of cytoplasmic Ca^{2+}. The dependence on both voltage and Ca^{2+} makes BK channels central to cellular processes that involve both Ca^{2+} signaling and membrane voltage changes. These include smooth muscle contraction, frequency tuning of sensory hair cells, and regulation of neurotransmitter release (*1*−*5*). Previous studies have revealed that voltage and Ca^{2+} activate BK channels through distinct mechanisms (*6*, *7*). BK channels possess intrinsic voltage sensors that induce channel opening in response to membrane depolarization and can be activated by voltage in the absence of Ca^{2+} binding (*6*, *8*−*12*). Ca^{2+} modulates the kinetic and steady-state responses of the channel to voltage by shifting the voltage dependence of the steady-state open probability (P_o) and the activation time constants to a more negative voltage range (*6*, *7*, *13*−*16*). Both voltage-dependent and Ca^{2+}-dependent activation of the channel involve allosteric mechanisms (*6*, *7*) that are individually well described by Monod−Wyman−Changeux (MWC) type models for allosteric proteins (*7*, *10*, *11*, *15*, *17*).

The primary structure of cloned *slo* channels is consistent with separate Ca^{2+}- and voltage-dependent activation mechanisms. Alignment of the amino acid sequences revealed similarities between a core domain of *slo* channels and voltage-gated K^+ channels (*16*, *18*−*21*). This core domain contains putative transmembrane segments S1−S6 that are conserved in voltage-gated K^+ channels (*22*−*24*). In particular, the S4 segment that has repeated and regularly spaced basic residues is part of the voltage sensor in voltage-gated K^+ channels (*25*−*29*). The remaining sequences, S0 and the large C-terminal tail domain, are unique and well conserved among various *slo* channels (*16*, *18*−*20*, *30*). This structural arrangement of the *slo* channel protein has led to a hypothesis that the core domain is responsible for its voltage dependence and the C-terminal domain is responsible for its Ca^{2+} sensing. Several studies have lent strong experimental support to this hypothesis (*21*, *31*−*33*).

Although voltage and Ca^{2+} activate BK channels through distinct molecular mechanisms, they influence each other's ability to activate the channel. The voltage dependence of the steady-state and kinetic properties of BK channels shifts to a more negative range with increasing $[Ca^{2+}]_i$ (*6*, *9*, *14*−*16*, *19*, *20*, *34*, *35*). Likewise, the channels' apparent affinity for Ca^{2+}, estimated from steady-state conductance measurements, is higher at more positive voltages (*6*, *14*). Therefore, the response of the channel protein to one stimulus (voltage or calcium) depends on its state, which is influenced by the other stimulus. The molecular mechanism underlying this interaction between voltage and Ca^{2+} during channel activation is not clear. Because measurable properties of channel gating depend on the linkage between Ca^{2+} binding, voltage sensor activation, and channel opening, it is difficult to distinguish the relative contributions of Ca^{2+}- and voltage-

† This work was supported by a National Institute of Mental Health Silvio Conte Center for Neuroscience Research Grant (MH 48108 to R.W.A.) and a grant from the American Heart Association (9930025N to J.C.). R.W.A. is an investigator with the Howard Hughes Medical Institute.

* To whom correspondence should be addressed. Phone: (216)368-0657. Fax: (216)368-4969. E-mail: jxc93@po.cwru.edu.

‡ Case Western Reserve University.

§ Stanford University.

[1] Abbreviations: BK channels, large conductance Ca^{2+}-activated K^+ channels; $[Ca^{2+}]_i$, intracellular calcium concentration; mutants of mslo1 are designated by the wild-type amino acid residue, the sequence number, and the amino acid to which the residue was mutated.

10.1021/bi001509+ CCC: $19.00
Published on Web 11/23/2000

dependent gating mechanisms to changes in open probability. For example, mutation of structures that presumably underlie Ca^{2+} binding often changes the channels' apparent voltage dependence (*32*) and vice versa (see Results). In this study, we investigate the mechanism that links the voltage and Ca^{2+} dependence of mslo1 channel activation by analyzing the effects of mutations in the S4 domain and its vicinity. Our results reveal that the free energy provided by voltage and Ca^{2+} in activating mslo1 channels are simply additive, ruling out the direct interaction between Ca^{2+} binding sites and voltage sensors. The linkage between the channel's voltage and Ca^{2+} dependence is allosteric in nature and is mediated by the conformational change between closed and open states of the channel.

MATERIALS AND METHODS

Clones, Mutagenesis, and Channel Expression. All experiments were performed on the mbr5 clone of the BK type Ca^{2+}-activated K^+ channel from mouse (mslo1) (*19*). To make site-directed mutations, we first introduced new restriction sites *Sal*I, *Bss*HII, *Bgl*II, *Spe*I, and *Afl*II at positions that flank the S4 or S5 region by PCR, which did not change the amino acid sequence (silent sites). The PCR product was verified by sequencing. The mutations in the S4 and S4−S5 linker regions were then generated by using synthesized sense and antisense oligonucleotides (29−75 nucleotides in length) containing the desired substitutions. These oligonucleotides were annealed and inserted into the mbr5 cDNA between our introduced restriction sites. The mutations were verified by multiple restriction digests.

Wild-type and mutant cRNA were transcribed in vitro using the "mMessage mMachine" kit with T3 polymerase (Ambion Inc., Austin, TX). A total of 0.05−0.5 ng of cRNA was injected into *Xenopus laevis* oocytes 2−6 days before recording. Currents from wild-type and mutant channels were always recorded on the same day and from the same batch of oocytes, although the channel properties did not vary significantly over the duration of the study or for different batches of injected oocytes.

Electrophysiology. Macroscopic currents were recorded from inside-out patches formed with borosilicate pipets of 1−2 MΩ resistance. Currents were less than 3 nA, and no series resistance compensation was applied. The pipet solution contained (mM) the following: 140 $KMeSO_3$, 20 Hepes, 2 KCl, and 2 $MgCl_2$, pH 7.20. The internal solution contained (mM) the following: 140 $KMeSO_3$, 20 Hepes, 2 KCl, and 1 HEDTA, pH 7.20, and was supplemented with 50 μM (+)-18-crown-6-tetracarboxylic acid to prevent Ba^{2+} block of the current (*36*, *37*). $CaCl_2$ was added to the internal solution to give the appropriate free $[Ca^{2+}]_i$, which was measured with a calcium-sensitive electrode. For $[Ca^{2+}]_i$ = 0.5 nM, the same internal solution was used except that HEDTA was substituted by 5 mM EGTA and no $CaCl_2$ was added. A sewer pipe flow system was used to supply the internal solution to the cytoplasmic face of the patch. Experiments were conducted at 23° C.

Very low open probabilities ($P_o \leq 10^{-3}$) were measured from macropatches containing several hundred mslo1 channels, as described previously (*10*). Since P_o was small ($\leq 10^{-3}$), single channel openings were observed. The corresponding all-points histograms were constructed, from which we obtained NP_o, where N is the total number of channels in the patch. The normalized open probability was determined by dividing NP_o by the maximum NP_o, which was obtained from macroscopic currents recorded in the same patch. Data acquisition and analysis were as described previously (*10*, *38*).

RESULTS

Activation Properties of the mslo1 Channel Are Altered by S4 Mutations. Is the Ca^{2+} modulation of mslo1 voltage-dependent gating due to a direct interaction between the voltage sensor and the Ca^{2+}-dependent machinery? We investigated this question by constructing three channels containing mutations in the S4 transmembrane segment or the S4−S5 linker: R207Q, R213Q, and E219R/Q222R. This section describes the effects of these mutations on mslo1 channel activation.

Like the wild-type mslo1 channel, the R207Q mutant channel was activated by depolarization, and the time course of activation was fit well by a single-exponential function (Figure 1A). The conductance versus voltage (G−V) relation of wild-type mslo1 channels and of R207Q mutant channels obtained at two different pairs of $[Ca^{2+}]_i$ are shown in Figure 1B. The G−V relations for both channel types were fit well by a Boltzmann function that shifted to the left on the voltage axis as the $[Ca^{2+}]_i$ was increased. The other mutant channels, E219R/Q222R and R213Q, were activated by voltage and Ca^{2+} in a similar way (Figure 2).

Figure 1 shows that the mutation R207Q changed the voltage dependence of mslo1 channel activation. The G−V relation of R207Q channels was shallower and shifted to the left of that for wild-type channels at all $[Ca^{2+}]_i$ examined. Under essentially calcium-free conditions ($[Ca^{2+}]_i \leq 0.5$ nM), the apparent equivalent gating charge (z) obtained from the Boltzmann fit to the G−V relation was more than two times smaller for R207Q channels as compared to wild-type channels. In addition, the half-maximal activation voltage ($V_{1/2}$) for R207Q channels was about 60 mV more negative than that for wild-type channels (Figure 1B, left). We showed previously that for calcium-free conditions, mslo1 channels are activated by voltage without binding Ca^{2+} (*6*). Therefore, the reduction of the equivalent gating charge and the shift in the G−V relation of R207Q channels in the absence of calcium indicates that the mutation altered the channels' voltage-dependent gating process.

The R207Q mutation also altered the magnitude of the G−V shift induced by an increase in $[Ca^{2+}]_i$. Increasing $[Ca^{2+}]_i$ from approximately 0 to 0.89 μM shifted the half-activation voltage by an amount $\Delta V_{1/2}$ that was more than twice as large for R207Q channels as for wild-type mslo1 channels (Figure 1B, left). Similar results were obtained when $[Ca^{2+}]_i$ was increased from 0.89 to 10.9 μM (Figure 1B, right). However, the equivalent gating charge (z) was significantly smaller for R207Q mutant channels than for the wild type. The averaged results for several cells show clearly that the R207Q mutation had reciprocal effects on z (Figure 1C, left) and $\Delta V_{1/2}$ (Figure 1C, middle). Interestingly, the product of the changes in z and $V_{1/2}$ due to an increase in $[Ca^{2+}]_i$, $\Delta(zV_{1/2})$, was not affected by the R207Q mutation for two different calcium concentration ranges (calcium free (~0.5 nM)−0.89 μM and 0.89−10.9 μM; Figure 1C, right).

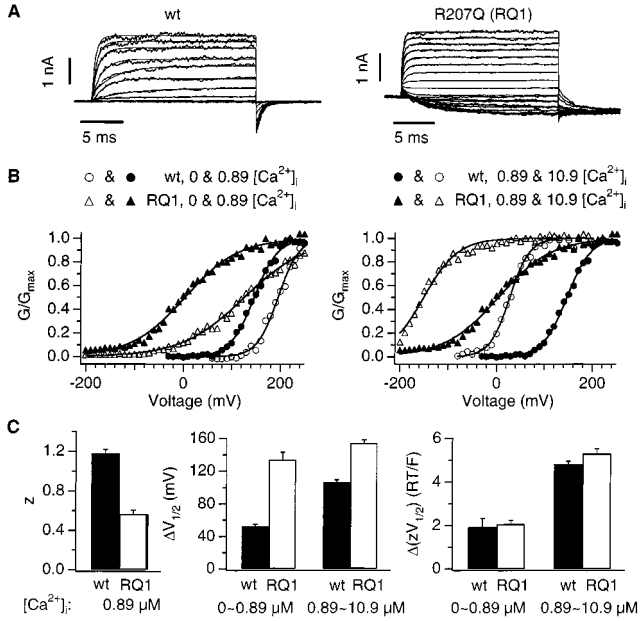

FIGURE 1: Voltage and Ca^{2+} dependence of the wild-type (wt) and the R207Q (RQ1) mslo1 channels. (A) Macroscopic currents in response to voltages −80 to +160 mV for wt and −200 to +160 mV for R207Q with 20-mV increments. The tail current potential was −80 mV. Solid thin curves show the fit with single-exponential functions. $[Ca^{2+}]_i$ was 10.9 μM. (B) Steady-state G−V relations were recorded at 0.5 nM (0) and 0.89 μM $[Ca^{2+}]_i$ (left) and at 0.89 and 10.9 μM $[Ca^{2+}]_i$ (right) as indicated on top of the plots. Relative conductance was determined from the tail current. The data were fitted with the Boltzmann function $G = G_{max}/(1 + \exp(-ze(V - V_{1/2})/kT))$ and then normalized to the maximum of the fit (solid lines). The parameters of the fits were as follows: (left) wt, $[Ca^{2+}]_i$ = 0.5 nM, z = 1.19, $V_{1/2}$ = 195.6 mV; $[Ca^{2+}]_i$ = 0.89 μM, z = 1.04, $V_{1/2}$ = 146.4 mV; R207Q, $[Ca^{2+}]_i$ = 0.5 nM, z = 0.40, $V_{1/2}$ = 126.0 mV; $[Ca^{2+}]_i$ = 0.89 μM, z = 0.46, $V_{1/2}$ = 3.2 mV. (right) The parameters of the fits at 0.89 μM $[Ca^{2+}]_i$ were the same as in the left graph, those at 10.9 μM $[Ca^{2+}]_i$ were as follows: wt, z = 1.25, $V_{1/2}$ = 27.4 mV; R207Q, z = 0.72, $V_{1/2}$ = −151.1 mV. (C) Averaged parameters from the fits. The parameters were obtained from the wt and R207Q (RQ1) at the $[Ca^{2+}]_i$ as indicated below the plots. $\Delta V_{1/2}$ = ($V_{1/2}$ at lower $[Ca^{2+}]_i$ − $V_{1/2}$ at higher $[Ca^{2+}]_i$) (middle) and $\Delta(zV_{1/2})$ = ($zV_{1/2}$ at lower $[Ca^{2+}]_i$ − $zV_{1/2}$ at higher $[Ca^{2+}]_i$) (right) were calculated from each patch and then averaged. Error bars represent the standard error of the mean from 6 to 8 patches.

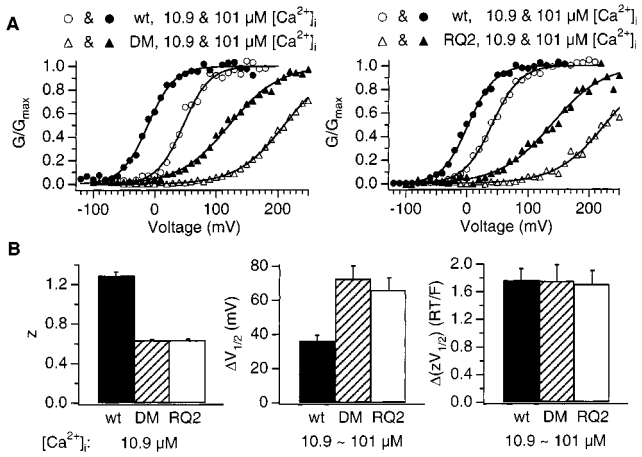

FIGURE 2: Voltage and Ca^{2+} dependence of the wt mslo1 (wt) and mutants E219R/Q222R (DM) and R213Q (RQ2). (A) Steady-state G−V relations for the wt and E219R/Q222R channels (left) and for the wt and R213Q channels (right) at 10.9 and 101 μM $[Ca^{2+}]_i$ as indicated at top of the plots. Solid lines are the fits of the Boltzmann function (see Figure 1 legend). The parameters of the fits were as follows: (left) wt, $[Ca^{2+}]_i$ = 10.9 μM, z = 1.19, $V_{1/2}$ = 46.8 mV; $[Ca^{2+}]_i$ = 101 μM, z = 1.19, $V_{1/2}$ = −10.8 mV; DM, $[Ca^{2+}]_i$ = 10.9 μM, z = 0.66, $V_{1/2}$ = 211.1 mV; $[Ca^{2+}]_i$ = 101 μM, z = 0.63, $V_{1/2}$ = 121.7 mV. (right) wt, $[Ca^{2+}]_i$ = 10.9 μM, z = 1.11, $V_{1/2}$ = 41.3 mV; $[Ca^{2+}]_i$ = 101 μM, z = 1.18, $V_{1/2}$ = 2.7 mV; R213Q, $[Ca^{2+}]_i$ = 10.9 μM, z = 0.64, $V_{1/2}$ = 226.4 mV; $[Ca^{2+}]_i$ = 101 μM, z = 0.61, $V_{1/2}$ = 138.6 mV. (B) Averaged parameters from the fits. The parameters were obtained from the wt, DM, and RQ2 channels at the $[Ca^{2+}]_i$ as indicated below the plots. Refer to Figure 1 legend for the methods in obtaining $\Delta V_{1/2}$ and $\Delta(zV_{1/2})$ and the meaning of error bars.

The E219R/Q222R double mutant (Figure 2A, left) and the R213Q point mutant (Figure 2A, right) also reduced the slope of the G−V relation at each $[Ca^{2+}]_i$ examined, including calcium-free solution. Like R207Q (Figure 1), these mutations alter the voltage-dependent gating of mslo1 channels. The G−V relations of the double mutant and R213Q channels were shifted to more positive voltages as compared to the relation for wild-type channels (Figure 2A) and, thus, had the opposite effect of the R207Q mutation (Figure 1B). The current through the double mutant and R213Q mutant channels was very small in 0.5 nM $[Ca^{2+}]_i$, even at voltages as high as 250 mV (data not shown), consistent with the idea that the voltage range of their activation in the absence of Ca^{2+} was shifted to very positive voltages (also see ref *39*). The equivalent gating charge was smaller for both mutant channels than for wild-type channels (left, Figure 2B), but the mutant channels' G−V relations shifted more to the left on the voltage axis in response to a given increase in $[Ca^{2+}]_i$ than that of wild-type mslo1 channels (Figure 2A). Similar to the results shown above for R207Q and wild-type channels (Figure 1C), Δz and $\Delta V_{1/2}$ varied inversely for the double mutant and for R213Q channels (Figure 2B, left and middle), but their product remained constant (Figure 2B, right).

Our results demonstrate clearly that all three point mutations alter the voltage-dependent gating of mslo1 channels, as expected if the S4 domain is part of the voltage sensor. However, even though the mutations altered $\Delta V_{1/2}$ in response to a $[Ca^{2+}]_i$ increase, the data do not indicate directly whether the mutations also affect the channels' Ca^{2+}-dependent gating mechanism (Figures 1B and 2A). Changes in the Ca^{2+} dependence of the G−V relation were observed previously in *slo* channels as a result of mutations or the coexpression of α and β subunits (*9*, *21*, *30*, *32*, *40*−*50*). Although these changes are often interpreted as effects on the channels' Ca^{2+} affinity, the Ca^{2+} dependence of the G−V relation is complexly determined by the voltage dependence, by the Ca^{2+} binding affinities of the channel in the open and closed states, and by interactions between the voltage sensors and the Ca^{2+} binding sites. As shown in the following, the reciprocal relationship between Δz and $\Delta V_{1/2}$ indicates that the effects of the mutations on the Ca^{2+} dependence of the G−V relation are consequences of the altered voltage dependence of channel activation. Even though the S4 mutations enhanced the channels' response to a change in $[Ca^{2+}]_i$, they did not appear to alter the channels' Ca^{2+}-dependent gating mechanism.

Energetic Additivity between Voltage and Calcium-Dependent Activation. Our previous results demonstrated that the G−V relation of the wild-type mslo1 channels could be

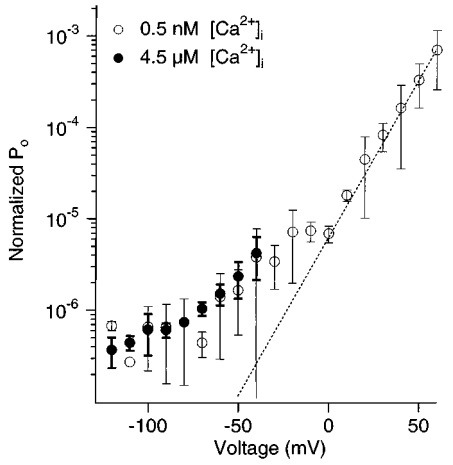

FIGURE 3: Voltage dependence of the open probability of the wild-type mslo1 channels for $P_o \leq 10^{-3}$. Normalized P_o from nine patches measured at 0.5 nM $[Ca^{2+}]_i$ was obtained as described in Methods and then averaged. NP_o measured at 4.5 μM $[Ca^{2+}]_i$ was scaled to the P_o measured at 0.5 nM $[Ca^{2+}]_i$ by multiplying by a constant factor, which made the value measured at -80 mV to be equal. The scaled NP_o measured at 4.5 μM $[Ca^{2+}]_i$ from seven patches were then averaged and plotted. The error bars represent the standard deviation. The error bars in bold are for the results for 4.5 μM $[Ca^{2+}]_i$.

fit by the Boltzmann equation at all $[Ca^{2+}]_i$, whereas the activation and deactivation kinetics could be fit by a single exponential (*6*). The results shown above indicate that these properties remain the same in mutant mslo1 channels. Therefore, the open probability of mslo1 channels can be aproximated by

$$P_o = \frac{1}{1 + \exp(\Delta G_{V,Ca}/kT)} \quad (1)$$

where k is Boltzmann's constant, T is the absolute temperature, and $\Delta G_{V,Ca}$ is the free energy change of channel opening. The expression of $\Delta G_{V,Ca}$ depends on the specific mechanism considered to describe the mslo1 channel activation, of which the most currents involve multiple open and closed states (*7*, *10*, *51*). For models with multiple open and closed states, the $\Delta G_{V,Ca}$ in general is a complex function of voltage and $[Ca^{2+}]_i$. However, as explained in the following, the results in Figure 3 show that for the mslo1 channel $\Delta G_{V,Ca}$ can be expressed by

$$\Delta G_{V,Ca} = \Delta G_V + \Delta G_{Ca} \quad (2)$$

where ΔG_V is the free energy change with voltage, resulting from the free energy changes of the voltage sensor in the open and closed conformations of the protein in the electrical field, and ΔG_{Ca} is the "chemical" part of the free energy change, resulting from Ca^{2+} binding and the internal free energy of opening (*52*). Since Ca^{2+} binding is not voltage dependent (*6*), ΔG_{Ca} does not change with varying voltages.

Figure 3 shows the voltage dependence of the open probability of wild-type mslo1 channels at very negative voltages, where $P_o \leq 3 \times 10^{-3}$. Under such conditions, eq 1 becomes

$$\log(P_o) = -\frac{\Delta G_{V,Ca}}{2.302kT} \quad (3)$$

We showed previously that the voltage dependence of log(P_o) for mslo1 channels does not reach a constant "limiting" slope at negative voltages as expected for a simple Boltzmann function. Instead, the slope of the voltage dependence decreased as the voltage became more negative (*10*). This effect is evident at both calcium-free (0.5 nM) and 4.5 μM $[Ca^{2+}]_i$, even though P_o was about 10^3 larger at 4.5 μM $[Ca^{2+}]_i$ than at 0.5 nM $[Ca^{2+}]_i$ (*10*). In Figure 3, the P_o measured at 4.5 μM $[Ca^{2+}]_i$ is multiplied by a constant scaling factor so that at each voltage it is reduced by about 10^3 to compare with that measured at 0.5 nM $[Ca^{2+}]_i$. Equation 3 predicts that if $\Delta G_{V,Ca}$ can be expressed by eq 2, the voltage dependence of log(P_o) at 0.5 nM $[Ca^{2+}]_i$ will be the same as the scaled log(P_o) at 4.5 μM $[Ca^{2+}]_i$ because a change in the $[Ca^{2+}]_i$ only changes ΔG_{Ca}, which is not voltage dependent. On the other hand, if $\Delta G_{V,Ca}$ is a function whereby voltage- and Ca^{2+}-dependent component of $\Delta G_{V,Ca}$ cannot be separately expressed by additive terms of ΔG_V and ΔG_{Ca}, the voltage dependence of log(P_o) would be unlikely the same at 0.5 nM and 4.5 μM $[Ca^{2+}]_i$, sufficient to alter P_o by a large factor of 10^3. In mathematical terms, eq 3 predicts that d[log(P_o)]/dV does not depend on $[Ca^{2+}]_i$ only if eq 2 is true. Figure 3 shows that the voltage dependence of the scaled log(P_o) measured at 4.5 μM $[Ca^{2+}]_i$ essentially superimposes on that measured at 0.5 nM $[Ca^{2+}]_i$, indicating that $\Delta G_{V,Ca}$ can be expressed by additive terms of ΔG_V and ΔG_{Ca} as in eq 2.

The energetic additivity shown in eq 2 indicates that for mslo1 channels the electrical and the Ca^{2+} binding free energies can compensate for each other to sustain the channel open probability. For example, to maintain $P_o = 0.5$, the change in the Ca^{2+} binding contribution to the ΔG of opening as a result of a $[Ca^{2+}]_i$ increase, $\Delta\Delta G_{Ca}$, must exactly counterbalance any change in the electrical component of the free energy:

$$\Delta\Delta G_V = -\Delta\Delta G_{Ca} \quad (4)$$

We have approximated the electrical energy by fitting the G$-$V relation to a Boltzmann equation (Figure 1). Therefore, at $P_o = 0.5$:

$$\Delta G_V = -zeV_{1/2} \quad (5)$$

where e is the elementary charge. The energetic additivity results in a relationship:

$$\Delta(zeV_{1/2}) = -\Delta\Delta G_{Ca} \quad (6)$$

which underlies the shift of the G$-$V relation on the voltage axis with various $[Ca^{2+}]_i$ for the wild-type and mutant mslo1 channels. More importantly, eq 6 also indicates that $\Delta(zV_{1/2})$ is a direct measure of the change in the Ca^{2+} binding contribution to the ΔG of opening in response to a $[Ca^{2+}]_i$ increase.

As shown in Figures 1 and 2, all three mutations reduced the G$-$V slope at each $[Ca^{2+}]_i$, including calcium-free conditions. Therefore, these mutations must have affected the free energy change with voltage, ΔG_V. However, since none of the three mutations alter $\Delta(zV_{1/2})$ (Figures 1C and 2B), the mutations do not affect the change in the Ca^{2+} binding contribution to the ΔG of opening, $\Delta\Delta G_{Ca}$, in response to a $[Ca^{2+}]_i$ increase. $\Delta\Delta G_{Ca}$ depends on the

mechanism by which Ca^{2+} binding changes the channel conformation during activation and is a function of the Ca^{2+} affinities of the various channel conformations. For example, for gating by the voltage-dependent MWC mechanism (*7*):

$$\Delta\Delta G_{Ca} = -4kT\,\Delta\left\{\ln\left[\frac{1+\frac{[Ca]_i}{K_C}}{1+\frac{[Ca]_i}{K_O}}\right]\right\} \qquad (7)$$

where K_C and K_O are the microscopic Ca^{2+} dissociation constants for each subunit when the channel is in the closed and open conformation, respectively (Scheme 1). Since none of the three mutations affect $\Delta\Delta G_{Ca}$, we conclude that the mutations did not alter the molecular properties of Ca^{2+}-dependent activation.

Allosteric Mechanism of Voltage- and Ca^{2+}-Dependent Activation. Taken together, our analysis shows that all three mutations altered the voltage dependence of mslo1 channel activation without affecting the mechanism of the Ca^{2+} dependence. This conclusion provides a molecular interpretation for the synergistic effects of voltage and Ca^{2+} on channel activation. The modulation of the voltage-dependent activation by Ca^{2+} cannot be due to a direct interaction between the residues Q207, R213, E219, or Q222 and the calcium-dependent machinery through physical contacts or electrostatic interactions. If so, then the structural and charge perturbations caused by their mutations would have altered such direct interactions, thereby affecting the Ca^{2+}-dependent activation (*53*−*55*). Since these residues nearly span the entire S4 region, it is likely that the linkage between the voltage and Ca^{2+} dependence of mslo1 channel activation is not derived from a direct interaction between the voltage sensors and the Ca^{2+}-dependent machinery. As we will show in the following, this conclusion is consistent with our current understanding of the voltage- and Ca^{2+}-dependent mechanisms of mslo1 channel activation.

The mslo1 channels are homotetramers (*56*). Each subunit contains a voltage-sensing S4 domain (*16*, *18*, *20*, *21*) and a Ca^{2+} binding site (*33*). Ca^{2+} activates the channel in a highly cooperative fashion (*6*, *7*). Such a mechanism has been described by models (*7*, *15*) drawn from the cyclic allosteric MWC scheme (*17*).

Scheme 1

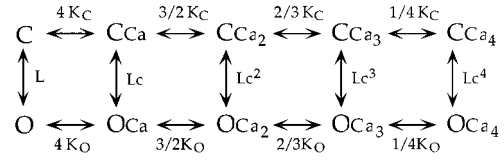

In Scheme 1, the opening of the channel alters the Ca^{2+} binding sites, resulting in a higher Ca^{2+} affinity for open (O) as compared to closed (C) channels. The binding of each Ca^{2+} promotes channel opening by changing the equilibrium between O and C, (L), by the factor c (K_O/K_C).

While this model can account for Ca^{2+}-dependent activation of the mslo1 channel over a wide range of conditions (*7*, *15*) it oversimplifies the voltage-dependent activation by assuming a single concerted voltage-dependent transition between the closed and the open conformations. Upon a closer examination of the macroscopic current and gating current of the mslo1 channel in the virtual absence of Ca^{2+}, Horrigan et al. (*10*, *11*) discovered that the voltage-dependent activation involved rapid movements of the voltage sensor in each of four subunits as well as a concerted C−O transition among all the subunits (also see ref *35*). While the activation of voltage sensors in each subunit promoted the channel opening, it was not required. The channel could open even when no voltage sensor had moved, but the channel opening facilitated the voltage sensor movements (*10*, *11*). These findings indicated that the voltage sensor movements activated the channel through an allosteric interaction, which could be described by a model resembling the MWC scheme (Scheme 2) (*10*).

Scheme 2

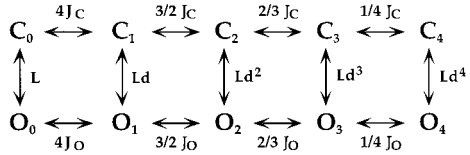

In Scheme 2, the horizontal transitions represent the voltage sensor movements in subunits. Their equilibrium constants are J_C and J_O at C and O conformations, respectively, and $d = J_O/J_C$.

It is striking that a similar allosteric mechanism can describe separately both voltage- and Ca^{2+}-dependent activation of the mslo1 channel. Taking these results together, it is reasonable to conclude that the mslo1 channel undergoes a quaternary conformational change between closed and open states that is concerted among all four subunits. Either the activation of the voltage sensor or the binding of Ca^{2+} in each subunit would affect this conformational change by favoring the open conformation. The simplest model to describe this mechanism is Scheme 3, shown in Figure 4A, which combines the calcium-dependent gating model of Scheme 1 with the voltage-dependent gating model of Scheme 2 (see also ref *43*). In Scheme 3 (shown in Figure 4A), the binding of Ca^{2+} is represented by horizontal transitions parallel to the page, where K_d is equivalent to K_C in Scheme 1 with no voltage sensor activated. The voltage sensor movements are represented by transitions perpendicular to the page, where $K(V)$ is equivalent to J_C in Scheme 2 with no Ca^{2+} bound. The subscript for each C or O state, *mn*, indicates the number of voltage sensors activated (m) and the number of Ca^{2+} bound (n). Only some of the 25 closed states are shown for clarity. The C−O transitions are also weakly voltage dependent (*10*, *11*) and are allosterically modulated by the movement of voltage sensors as well as the binding of Ca^{2+}. The activation of each voltage sensor alters the equilibrium of the C−O transition by a factor d, whereas each Ca^{2+} binding event changes this equilibrium by a factor c:

$$L(V)_{m,n} = d^m c^n L(V) \quad m, n = 0-4 \qquad (8)$$

where $L(V)$ is the equilibrium constant for the C−O transition when the channel has no voltage sensor activated and no Ca^{2+} bound.

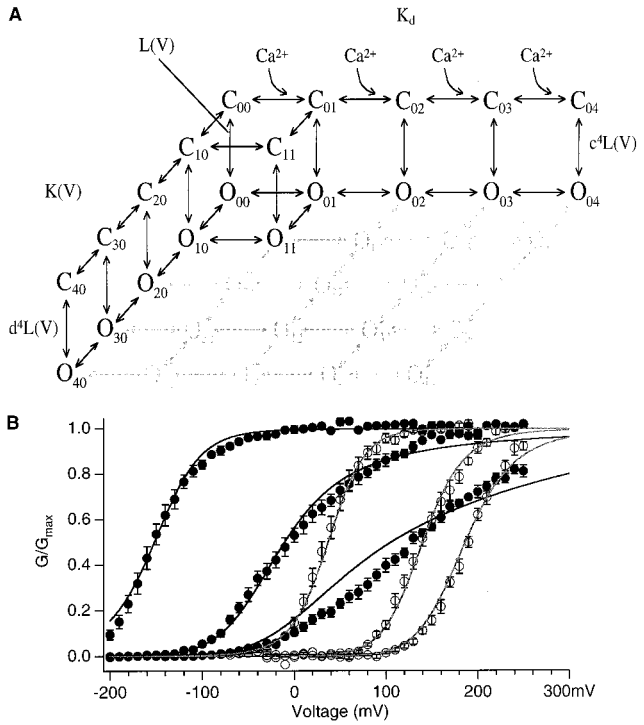

FIGURE 4: (A) Scheme 3. Parameters are described in the text. Not all of the closed states and transitions are shown in the interest of clarity. (B) The fit of Scheme 3 to the data obtained from wild-type mslo1 (open circles) and R207Q (filled circles). For both channels, steady-state G−V relations were measured at $[Ca^{2+}]_i$ (from right to left) of 0.5 nM, 0.89 μM, and 10.9 μM and then averaged. Error bars represent the standard error of the mean. The number of patches represented in the graph is 8−11 for wild-type mslo1 and 6−8 for R207Q. The smooth curves are the fits with parameters as follows: wt, $K_d = 1.6 \times 10^{-5}$ M, $c = 12.5$, $K(V) = \exp(0.375e(V - 160)/kT)$, $d = 15$, $L(V) = 7 \times 10^{-6} \exp(0.4\text{ eV}/kT)$, $g = 1$; R207Q, $K_d = 1.6 \times 10^{-5}$ M, $c = 12.5$, $K(V) = \exp(0.42e(V + 50)/kT)$, $d = 10$, $L(V) = 7 \times 10^{-5} \exp(0.15\text{ eV}/kT)$, $g = 1$.

The channel open probability for Scheme 3 (shown in Figure 4A) follows eq 1 with

$$\Delta G_{V,Ca} = kT \ln\left\{\frac{1}{L(V)}\left\{\left(1 + \frac{[Ca]_i}{K_d}\right)^4 + 4K(V)\left(1 + g\frac{[Ca]_i}{K_d}\right)^4 + 6K(V)^2\left(1 + g^2\frac{[Ca]_i}{K_d}\right)^4 + 4K(V)^3\left(1 + g^3\frac{[Ca]_i}{K_d}\right)^4 + K(V)^4\left(1 + g^4\frac{[Ca]_i}{K_d}\right)^4\right\}\Bigg/ \left\{\left(1 + \frac{[Ca]_i}{cK_d}\right)^4 + 4dK(V)\left(1 + g\frac{[Ca]_i}{cK_d}\right)^4 + 6d^2K(V)^2\left(1 + g^2\frac{[Ca]_i}{cK_d}\right)^4 + 4d^3K(V)^3\left(1 + g^3\frac{[Ca]_i}{cK_d}\right)^4 + d^4K(V)^4\left(1 + g^4\frac{[Ca]_i}{cK_d}\right)^4\right\}\right\} \quad (9)$$

The factor g describes the interaction between the voltage sensors and Ca^{2+} binding. For simplicity, we have assumed that binding of Ca^{2+} to one subunit affects the voltage sensors in all four subunits equally by the factor g. Interactions between only neighboring subunits would require additional states and more complex mathematics; however, the same basic findings would still apply. According to eq 9, if the voltage sensor directly interacts with the Ca^{2+}-dependent machinery, the voltage sensor movements will be altered with each additional Ca^{2+} bound. Reciprocally, activation of each voltage sensor will effect the binding of Ca^{2+}. Such a direct interaction could occur between the voltage sensor and Ca^{2+} dependent machinery within the same subunit or from different subunits. The allosteric effects of voltage sensor movements and Ca^{2+} binding, combined with the possible direct interaction between voltage sensors and the Ca^{2+}-dependent machinery in Scheme 3 result in a complex dependence of $\Delta G_{V,Ca}$ on voltage and calcium concentration (eq 9). With such a complex dependence, the energy provided by voltage and by calcium binding are generally not additive and $\Delta(zV_{1/2})$ will not generally be constant, a prediction that is inconsistent with our experimental results. However, if the Ca^{2+}-dependent machinery does not directly interact with voltage sensors (i.e., when $g = 1$), energetic additivity will be observed. In such a case

$$\Delta G_{V,Ca} = \Delta G^I_V + \Delta G^I_{Ca} \quad (10)$$

where

$$\Delta G^I_V = kT \ln\left\{\frac{1}{L(V)}\left(\frac{1 + K(V)}{1 + dK(V)}\right)^4\right\} \quad (11)$$

and

$$\Delta G^I_{Ca} = 4kT \ln\left(\frac{1 + \frac{[Ca]_i}{K_d}}{1 + \frac{[Ca]_i}{cK_d}}\right) \quad (12)$$

Thus, when interpreted in terms of this more realistic model of calcium- and voltage-dependent gating, our results support the hypothesis that the voltage sensor movements and Ca^{2+} binding both activate the mslo1 channel by an allosteric mechanism without affecting each other directly. The apparent effects of $[Ca^{2+}]_i$ on the voltage dependence of the channel and the effects of voltage on the Ca^{2+} dependence (6) occur through an allosteric mechanism mediated by the conformational change between the open and closed states of the channel.

DISCUSSION

We have studied three mutations in the putative S4 or S4−S5 linker regions in the mslo1 channel to explore the relationship between voltage and Ca^{2+} in activating the channel. All three mutations changed channel activation in two main respects: first, the G−V relations shifted along the voltage axis and their slopes were reduced; second, the G−V shift induced by a given change in $[Ca^{2+}]_i$ was increased. These two effects were inversely related: the Ca^{2+} induced G−V shift increased with the same proportion as the reduction of the G−V steepness, even though the three mutations had distinct effects on the channel's voltage dependence (Figures 1 and 2). These results indicate that

although the voltage-dependent mechanism of channel activation was altered by the mutations, the mechanism that links the voltage dependence and Ca^{2+} dependence remained intact. Thus, this linkage cannot be due to a direct interaction between the voltage sensor and the Ca^{2+}-dependent machinery. We conclude that it is an allosteric linkage, i.e., the voltage and Ca^{2+} dependence are linked through the conformational change between the closed and the open channel (*57*). Such a mechanism resembles the well-known allosteric regulation of hemoglobin by 2,3-diphosphoglycerate (DPG) and oxygen, in which DPG binding to the deoxyhemoglobin stabilizes its conformation and thereby lowers the oxygen affinity of hemoglobin (*58*).

The allosteric linkage between voltage- and Ca^{2+}-dependent activation of the mslo1 channel is consistent with the channel structure that the voltage sensor and Ca^{2+} binding site are in two separable domains (*21*, *33*). However, our current structural knowledge alone does not obviate the possiblity that the two domains may be associated in a way that the Ca^{2+} binding site is so close to the voltage sensor that a bound Ca^{2+} may facilitate the movement of the voltage sensor by physical contact or by affecting the local electrical field. These possibilities are now excluded in this study by two lines of independent evidence: (i) the mutations on the voltage sensor do not alter the mechanism of Ca^{2+}-dependent activation; and (ii) the energies provided by voltage and by Ca^{2+} binding are additive in activating the channel, whereas no free energy changes due to the direct interaction of voltage sensor and Ca^{2+} binding are observed. An example of such an allosteric mechanism is provided in Scheme 3 where the factor g must equal to 1 in order to describe the voltage- and Ca^{2+}-dependent activation of mslo1 channels. In recent studies of single BK channels over a range of $[Ca^{2+}]_i$ and voltage, Rothberg and Magleby (*51, 59*) found that the channel gated among multiple closed and open states in a Ca^{2+}-independent fashion and through two or more independent transition pathways between closed and open states. These findings led them to propose a two-tiered model that is similar to Scheme 3. The similarity between their model and Scheme 3 together with their conclusion support a lack of direct intreractions between the voltage sensors and the Ca^{2+} binding sites.

Previous studies have revealed that the separate activation of BK channels by Ca^{2+} and by voltage occurs through an allosteric mechanism (*6, 7, 10, 11, 51*). Although they used an oversimplified voltage dependence, models drawn from the MWC scheme (*7, 15*) successfully described the Ca^{2+} dependent activation of wild-type BK channels. Nevertheless, the MWC scheme is no longer adequate to describe the activation of our mutant channels. As shown in Figure 1B, the G−V relation of the R207Q mutant channel became more steep with increasing $[Ca^{2+}]_i$. The equivalent gating charge of the R207Q mutant channel measured at 10.9 μM $[Ca^{2+}]_i$ ($z = 0.89 \pm 0.04$) was more than twice as large as that measured at 50 nM $[Ca^{2+}]_i$ ($z = 0.38 \pm 0.02$). The change in the slope of the G−V relations of wild-type mslo1 channels with $[Ca^{2+}]_i$ is inconsistent with the MWC model prediction (*6, 7*), but the change was so small that the MWC model could describe the mslo1 activation at the macroscopic current level fairly well within experimental variability (*7*). Such a slope change is required by Scheme 3, and derives from the fact that the voltage dependence of the channel is determined by two voltage dependent processes: the voltage sensor movements and the C−O transitions. The contribution of the C−O transition, which has a weaker voltage dependence than the voltage sensor movements, varies over the voltage range (*10*). Therefore, the G−V relation at a low $[Ca^{2+}]_i$ has a shallower slope because of its positive voltage range (Figure 1). Since the mutation R207Q changed the voltage sensor movements as well as their relationship with the C−O transitions, the change of the G−V slope at various $[Ca^{2+}]_i$ is made more prominent (*10*). Figure 4B shows a Scheme 3 simulation of the G−V relations of wild-type and the R207Q mutant channels. The model reproduces the general effect of the mutation on the activation of mslo1 channels, including the shift of the G−V relation, the slope change at various $[Ca^{2+}]_i$, and the reciprocal relationship between the increase in the calcium-induced shift of the G−V relations and the reduction in their slope.

While it is clear that the mutations described in this paper altered the voltage-dependent gating of mslo1 channels, the mechanism underlying these alterations is uncertain. The mutations shifted the G−V relations on the voltage axis and reduced their steepness. However, in general neither the changes in the slope of these relations nor the changes in side chain charges are related in a simple way to possible changes in the valence of the gating charge associated with channel activation (*10, 11, 27, 28, 60*). Rather, the equivalent charge obtained from our Boltzmann fits to the G−V relations represents an empirical measure of the steepness of the curves and is not a measure of the true gating charges. Since the voltage dependence of $\log(P_o)$ for mslo1 channels did not reach a "limiting slope" at negative voltages (Figure 3), these results also do not provide an estimate for the valence of the gating charge (*61*). Figure 4B shows the fit of Scheme 3 to the G−V relations of wild-type and R207Q mutant mslo1 channels. Our data are not sufficient to ensure that the model used in the fits represents an accurate description of the activation mechanism, but they do suggest that the mutation may have altered many voltage-dependent transitions, including voltage sensor movements in individual subunits and cooperative transitions leading to channel opening.

In contrast to our conclusions, Diaz et al. (*39*) have suggested that mutations in the *hslo* S4 region, including R207Q, R213Q, and E219K, mainly affected calcium-dependent activation by altering the calcium affinities of both open and closed states. They reached this conclusion by fitting the $V_{1/2} - [Ca^{2+}]_i$ relation with an equation derived from the MWC model. A fixed equivalent gating charge estimated from the G−V relation at a single $[Ca^{2+}]_i$ for each mutation was used in their fits. As discussed above, equivalent gating charge, determined from the slope of the G−V relations, for the mutant channels, particularly R207Q, changed with $[Ca^{2+}]_i$. Therefore, the equivalent gating charge estimated from the G−V relation varied with $V_{1/2}$. In this respect the MWC model is not adequate to describe the behavior of mutant channels because it does not produce $[Ca^{2+}]_i$-dependent changes in the slope of the G−V relations. However, the slope change of G−V relation with $[Ca^{2+}]_i$ for the R207Q channel was not observed by Diaz et al. because they reported the G−V relation only at a single $[Ca^{2+}]_i$. We believe that the discrepancy between our conclusion and the conclusion by Diaz et al. (*39*) regarding

the effect of S4 mutations on calcium binding mainly arises from this difference in treatment of the results.

ACKNOWLEDGMENT

The mslo1 clone was kindly provided to us by Dr. Larry Salkoff. We thank Richard Tsien, Frank Horrigan, Tom Middendorf, and Stephen Jones for helpful comments on the manuscript.

REFERENCES

1. Hudspeth, A. J., and Lewis, R. S. (1988) *J. Physiol.* (*London*) *400*, 237−74.
2. Hudspeth, A. J., and Lewis, R. S. (1988) *J. Physiol.* (*London*) *400*, 275−97.
3. Robitaille, R., Garcia, M. L., Kaczorowski, G. J., and Charlton, M. P. (1993) *Neuron 11*, 645−55.
4. Nelson, M. T., Cheng, H., Rubart, M., Santana, L. F., Bonev, A. D., Knot, H. J., and Lederer, W. J. (1995) *Science 270*, 633−7.
5. Wu, Y. C., Art, J. J., Goodman, M. B., and Fettiplace, R. (1995) *Prog. Biophys. Mol. Biol. 63*, 131−58.
6. Cui, J., Cox, D. H., and Aldrich, R. W. (1997) *J. Gen. Physiol. 109*, 647−73.
7. Cox, D. H., Cui, J., and Aldrich, R. W. (1997) *J. Gen. Physiol. 110*, 257−81.
8. Pallotta, B. S. (1985) *J. Gen. Physiol. 86*, 601−11.
9. Meera, P., Wallner, M., Jiang, Z., and Toro, L. (1996) *FEBS Lett. 382*, 84−8.
10. Horrigan, F. T., Cui, J., and Aldrich, R. W. (1999) *J. Gen. Physiol. 114*, 277−304.
11. Horrigan, F. T., and Aldrich, R. W. (1999) *J. Gen. Physiol. 114*, 305−36.
12. Talukder, G., and Aldrich, R. W. (2000) *Biophys. J. 78*, 761−72.
13. Marty, A. (1981) *Nature 291*, 497−500.
14. Pallotta, B. S., Magleby, K. L., and Barrett, J. N. (1981) *Nature 293*, 471−4.
15. McManus, O. B., and Magleby, K. L. (1991) *J. Physiol.* (*London*) *443*, 739−77.
16. Adelman, J. P., Shen, K. Z., Kavanaugh, M. P., Warren, R. A., Wu, Y. N., Lagrutta, A., Bond, C. T., and North, R. A. (1992) *Neuron 9*, 209−16.
17. Monod, J., Wyman, J., and Changeux, J. P. (1965) *J. Mol. Biol. 12*, 88−118.
18. Atkinson, N. S., Robertson, G. A., and Ganetzky, B. (1991) *Science 253*, 551−5.
19. Butler, A., Tsunoda, S., McCobb, D. P., Wei, A., and Salkoff, L. (1993) *Science 261*, 221−4.
20. Tseng-Crank, J., Foster, C. D., Krause, J. D., Mertz, R., Godinot, N., DiChiara, T. J., and Reinhart, P. H. (1994) *Neuron 13*, 1315−30.
21. Wei, A., Solaro, C., Lingle, C., and Salkoff, L. (1994) *Neuron 13*, 671−81.
22. Papazian, D. M., Schwarz, T. L., Tempel, B. L., Jan, Y. N., and Jan, L. Y. (1987) *Science 237*, 749−53.
23. Kamb, A., Iverson, L. E., and Tanouye, M. A. (1987) *Cell 50*, 405−13.
24. Pongs, O., Kecskemethy, N., Muller, R., Krah-Jentgens, I., Baumann, A., Kiltz, H. H., Canal, I., Llamazares, S., and Ferrus, A. (1988) *EMBO J. 7*, 1087−96.
25. Larsson, H. P., Baker, O. S., Dhillon, D. S., and Isacoff, E. Y. (1996) *Neuron 16*, 387−97.
26. Mannuzzu, L. M., Moronne, M. M., and Isacoff, E. Y. (1996) *Science 271*, 213−6.
27. Aggarwal, S. K., and MacKinnon, R. (1996) *Neuron 16*, 1169−77.
28. Seoh, S. A., Sigg, D., Papazian, D. M., and Bezanilla, F. (1996) *Neuron 16*, 1159−67.
29. Yusaf, S. P., Wray, D., and Sivaprasadarao, A. (1996) *Pflugers Arch. 433*, 91−7.
30. Wallner, M., Meera, P., and Toro, L. (1996) *Proc. Natl. Acad. Sci. U.S.A. 93*, 14922−7.
31. Moss, G. W., Marshall, J., and Moczydlowski, E. (1996) *J. Gen. Physiol. 108*, 473−84.
32. Schreiber, M., and Salkoff, L. (1997) *Biophys. J. 73*, 1355−63.
33. Schreiber, M., Yuan, A., and Salkoff, L. (1999) *Nat. Neurosci. 2*, 416−21.
34. DiChiara, T. J., and Reinhart, P. H. (1995) *J. Physiol.* (*London*) *489*, 403−18.
35. Stefani, E., Ottolia, M., Noceti, F., Olcese, R., Wallner, M., Latorre, R., and Toro, L. (1997) *Proc. Natl. Acad. Sci. U.S.A. 94*, 5427−31.
36. Neyton, J. (1996) *Biophys. J. 71*, 220−6.
37. Diaz, F., Wallner, M., Stefani, E., Toro, L., and Latorre, R. (1996) *J. Gen. Physiol. 107*, 399−407.
38. Cox, D. H., Cui, J., and Aldrich, R. W. (1997) *J. Gen. Physiol. 109*, 633−46.
39. Diaz, L., Meera, P., Amigo, J., Stefani, E., Alvarez, O., Toro, L., and Latorre, R. (1998) *J. Biol. Chem. 273*, 32430−6.
40. McManus, O. B., Helms, L. M., Pallanck, L., Ganetzky, B., Swanson, R., and Leonard, R. J. (1995) *Neuron 14*, 645−50.
41. Brenner, R., Jegla, T. J., Wickenden, A., Liu, Y., and Aldrich, R. W. (2000) *J. Biol. Chem. 275*, 6453−61.
42. Meera, P., Wallner, M., and Toro, L. (2000) *Proc. Natl. Acad. Sci. U.S.A. 97*, 5562−7.
43. Wallner, M., Meera, P., and Toro, L. (1999) *Proc. Natl. Acad. Sci. U.S.A. 96*, 4137−42.
44. Behrens, R., Nolting, A., Reimann, F., Schwarz, M., Waldschutz, R., and Pongs, O. (2000) *FEBS Lett. 474*, 99−106.
45. Xia, X. M., Ding, J. P., and Lingle, C. J. (1999) *J. Neurosci. 19*, 5255−64.
46. Dworetzky, S. I., Boissard, C. G., Lum-Ragan, J. T., McKay, M. C., Post-Munson, D. J., Trojnacki, J. T., Chang, C. P., and Gribkoff, V. K. (1996) *J. Neurosci. 16*, 4543−50.
47. Nimigean, C. M., and Magleby, K. L. (2000) *J. Gen. Physiol. 115*, 719−36.
48. Cox, D. H., and Aldrich, R. W. (2000) *J. Gen. Physiol. 116*, 411−432.
49. Weiger, T. M., Holmqvist, M. H., Levitan, I. B., Clark, F. T., Sprague, S., Huang, W. J., Ge, P., Wang, C., Lawson, D., Jurman, M. E., Glucksmann, M. A., Silos-Santiago, I., DiStefano, P. S., and Curtis, R. (2000) *J. Neurosci. 20*, 3563−70.
50. Xia, X. M., Ding, J. P., Zeng, X. H., Duan, K. L., and Lingle, C. J. (2000) *J. Neurosci. 20*, 4890−903.
51. Rothberg, B. S., and Magleby, K. L. (1999) *J. Gen. Physiol. 114*, 93−124.
52. Labarca, P., Coronado, R., and Miller, C. (1980) *J. Gen. Physiol. 76*, 397−424.
53. Carter, P. J., Winter, G., Wilkinson, A. J., and Fersht, A. R. (1984) *Cell 38*, 835−40.
54. Ackers, G. K., and Smith, F. R. (1985) *Annu. Rev. Biochem. 54*, 597−629.
55. Wells, J. A. (1990) *Biochemistry 29*, 8509−17.
56. Shen, K. Z., Lagrutta, A., Davies, N. W., Standen, N. B., Adelman, J. P., and North, R. A. (1994) *Pflugers Arch. 426*, 440−5.
57. Colquhoun, D. (1998) *Br. J. Pharmacol. 125*, 924−47.
58. Kilmartin, J. V. (1976) *Br. Med. Bull. 32*, 209−12.
59. Rothberg, B. S., and Magleby, K. L. (2000) *J. Gen. Physiol. 116*, 75−100.
60. Zagotta, W. N., Hoshi, T., Dittman, J., and Aldrich, R. W. (1994) *J. Gen. Physiol. 103*, 279−319.
61. Sigg, D., and Bezanilla, F. (1997) *J. Gen. Physiol. 109*, 27−39.

BI001509+